The Journal of Infectious Diseases

BRIEF REPORT

Breakthrough Gastrointestinal COVID-19 and Intrahost Evolution Consequent to Combination Monoclonal Antibody Prophylaxis

Brandon J. Beddingfield,[1] Lori A. Rowe,[1] Kasi E. Russell-Lodrigue,[1] Lara A. Doyle-Meyers,[1] Nadia Golden,[1] Skye Spencer,[1] Nicole Chirichella,[1] Robert V. Blair,[1] Nicholas J. Maness,[1,2] and Chad J. Roy[1,2]

[1]Tulane National Primate Research Center, Covington, Louisiana, USA; and [2]Department of Microbiology and Immunology, Tulane School of Medicine, New Orleans, Louisiana, USA

Breakthrough gastrointestinal COVID-19 was observed after experimental SARS-CoV-2 upper mucosal infection in a rhesus macaque undergoing low-dose monoclonal antibody prophylaxis. High levels of viral RNA were detected in intestinal sites contrasting with minimal viral replication in upper respiratory mucosa. Sequencing of virus recovered from tissue in 3 gastrointestinal sites and rectal swab revealed loss of furin cleavage site deletions present in the inoculating virus stock and 2 amino acid changes in spike that were detected in 2 colon sites but not elsewhere, suggesting compartmentalized replication and intestinal viral evolution. This suggests suboptimal antiviral therapies promote viral sequestration in these anatomies.

Keywords. SARS-CoV-2; breakthrough infection; gastrointestinal tract; nonhuman primates; suboptimal prophylaxis.

The coronavirus disease 2019 (COVID-19) pandemic, caused by severe acute respiratory syndrome coronavirus 2 (SARS-CoV-2), has been the subject of much recent research regarding therapeutics and viral evolution [1]. A monoclonal antibody (mAb) therapy, produced by Regeneron, currently has emergency use authorization to be administered to COVID-19 patients relatively early in the course of disease, with successful results [2]. Other mAb-based therapies are currently under consideration as well, with one combination undergoing clinical trials (NCT04700163) targeting 2 separate locations within the receptor binding domain (RBD) of spike protein [3]. This mAb combination has been shown to protect prophylactically [4] and therapeutically [5] in a Rhesus macaque (*Macaca mulatta*; RM) model of SARS-CoV-2 infection, with viral loads in the respiratory and gastrointestinal tract significantly blunted.

Infection by SARS-CoV-2 has increasingly been seen as a gastrointestinal disease in addition to the typical respiratory disease it has been associated with since the start of the pandemic [6], with symptoms including nausea, vomiting, diarrhea, and abdominal pain present in 40% of infected individuals [7]. Intestinal damage has been noted during autopsy of individuals with fatal cases of disease [8], including viral protein detection in multiple locations [6]. Approximately 50% of patients admitted to hospitals for active disease exhibit digestive symptoms, with 5% of patients displaying digestive symptoms in the absence of respiratory complications [9].

Recently, the delta variant of SARS-CoV-2 (B.1.617.2) has outpaced other variants of concern to become dominant [10]. This was preceded by other variants including B.1.1.7 (alpha), B.1.351 (beta), and P.1 (gamma) [11]. Some of the sequence changes seen within these variants include those that aid in immune escape, such as those in E484 of spike RBD, which can lower neutralization capacity by more than an order of magnitude [12]. Mutations arising that display differential antibody binding properties are of significant concern for antibody therapeutic and prophylaxis approaches to combating the ongoing pandemic.

In this report, we focus on one RM, LT54, from a study that used a combination antibody therapy as a prophylaxis against SARS-CoV-2 infection [4]. We identified high levels of viral genome and subgenomic RNA within intestinal compartments after respiratory clearance. Intrahost evolution of virus was seen, with sequences changing in accordance with enhanced replication capacity, as well as site-specific differences potentially indicating preferential replication.

METHODS

Virus and Cells

Virus used for animal inoculation was strain SARS-CoV-2; 2019-nCoV/USA-WA1/2020 (BEI No. NR-52281) prepared on subconfluent VeroE6 cells (ATCC No. CRL-1586) and confirmed via sequencing. VeroE6 cells were used for live virus titration of biological samples and were maintained in Dulbecco's Modified Eagle's Medium (Thermo Scientific) with 10% fetal bovine serum.

Animals and Procedures

A total of 16 RMs (*Macaca mulatta*), between 3 and 11 years old, were utilized for this study. All RMs were bred in captivity at Tulane National Primate Research Center (TNPRC). The RMs were infused with 20, 6, or 2 mg/kg mAb cocktail 3 days

Received 16 November 2021; editorial decision 04 April 2022; accepted 12 April 2022; published online 16 April 2022

Correspondence: Chad J. Roy, PhD, Tulane National Primate Research Center, 18703 Three Rivers Road, Covington, LA 70447 (croy@tulane.edu).

The Journal of Infectious Diseases® 2022;226:1588–92

https://doi.org/10.1093/infdis/jiac134

before challenge. They were then exposed via intratracheal/intranasal installation of viral inoculum (1 mL intratracheal, 500 µL per nare, total delivery 2e+6 50% tissue culture infectious dose [$TCID_{50}$]).

The animals were monitored twice daily for the duration of the study, with collections of mucosal swabs (nasal, pharyngeal, rectal), as well as bronchioalveolar lavage, taken preexposure as well as postexposure days 1, 3, and at necropsy. Blood was collected preexposure, as well as days 1, 2, 3, 5, and at necropsy. Physical examinations were performed daily after exposure, and necropsy occurred between 7 and 9 days postexposure. During physical examination, rectal temperature and weight of each animal was performed. No animals met humane euthanasia endpoints during this study. During necropsy, tissues were collected in media, fresh frozen, or in fixative for later analysis.

Sample Collection and RNA Isolation

Swabs were collected in RNA/DNA Shield (Zymo Research). RNA was isolated using the Zymo Quick-RNA Viral kit, with the addition of the swab into the collection column to ensure complete removal of fluid. Bronchoalveolar lavage (BAL) cells and tissues were collected in Trizol, tissues were homogenized, and RNA was isolated using a RNeasy Mini Kit (No. 74106; Qiagen) after phase separation with chloroform.

Quantification of Viral RNA Using Quantitative Real-Time PCR

Isolated RNA was analyzed in a QuantStudio 6 (Thermo Scientific) using TaqPath master mix (Thermo Scientific) and appropriate primers/probes [4] with the following program: 25°C for 2 minutes, 50°C for 15 minutes, 95°C for 2 minutes followed by 40 cycles of 95°C for 3 seconds and 60°C for 30 seconds. Signals were compared to a standard curve generated using in vitro transcribed RNA of each sequence diluted from 10^8 down to 10 copies. Positive controls consisted of SARS-CoV-2–infected VeroE6 cell lysate. Viral copies per swab or BAL were calculated by multiplying mean copies per well by volume in the total swab extract or BAL, while viral copies in tissue were calculated per microgram of RNA extracted from each tissue.

cDNA Conversion

cDNA was generated using Protoscript II (New England Biolabs) as follows: 10 µL template RNA, 1 µL 10 µM random hexamers, and 1 µL 10 mM dNTPs were incubated at 65°C for 5 minutes and then place directly on ice for 1 minute. The following was then added: 4 µL PSII buffer, 2 µL 100 mM DTT, 1 µL RNase inhibitor, and 1 µL PSII reverse transcriptase, and incubated at 42°C for 50 minutes, then 70°C for 10 minutes, followed by a hold at 4°C.

Sequencing

DNA libraries were made using the standard SWIFT Normalase Amplicon Panels protocol (SWIFT Biosciences) utilizing the SNAP UD indexing primers. The libraries were normalized to 4 nM and pooled. Paired-end sequencing (2 × 150) was performed on the Illumina MiSeq platform.

Data Analysis

Primer sequences were trimmed, and sequence reads were aligned to the SARS-CoV-2 genome (WA1/2020 isolate, accession MN985325) using the built-in mapping function in Geneious Prime software. Variants were called that were present at greater than 10% of reads at that site.

RESULTS

The animal that is the subject of this report (LT54) was a male Indian origin TNPRC purpose-bred and reared male approximately 4 years in age and a weight of 6.50 kg when assigned to the treatment study, both measures of which were comparable to other animals in the study cohort [4]. The only clinically remarkable aspect of this animal prior to assignment was a history of intermittent soft stool. Antibody combination (C-135-LS and C-144-LS, 2 mg/kg intravenous) was administered prophylactically 3 days before mucosal SARS-CoV-2 challenge. Clinical development of experimentally induced COVID-19 in this animal was generally mild. Daily veterinary physical examination yielded saturated blood oxygen measurements of >98% and auscultation within normal limits throughout disease course up until study termination and necropsy at day 7 postinfection. Transient sinus arrhythmia was noted day 2 postinfection. Mild anorexia early in COVID-19 infection resulted in negligible weight loss (approximately 6% of total body weight at termination of study). Viral loads via genomic (N gene) and subgenomic (E gene) RNA were followed for 1 week. Swab samples were acquired from pharyngeal, nasal, and rectum, as well as cells isolated from BAL fluid. In both real-time quantitative polymerase chain reaction (RT-qPCR) assays (genomic N and subgenomic E) viral loads in LT54 increased 1 to 2 days postinfection at respiratory sites, before resolving by necropsy at 7 days postinfection (Figure 1). Swab analysis showed near complete protection against replicating virus throughout the study, with subgenomic E analysis unable to detect virus in any respiratory site except pharyngeal (Figure 1). This indicates robust respiratory protection from challenge after prophylactic administration of antibodies.

This contrasts with viral RNA loads measured in the rectal site, seen as a delayed increase in relation to respiratory viral RNA trends that did not resolve by necropsy. Controls exhibited an increase at this site as well, though not to the extent of LT54 (Figure 1). Tissues collected at necropsy indicated complete protection in respiratory sites of LT54, with controls still exhibiting high amounts of viral RNA in almost all sites (Supplementary Figure 1A). The intestinal sites of LT54 showed the opposite pattern, with high amounts of viral

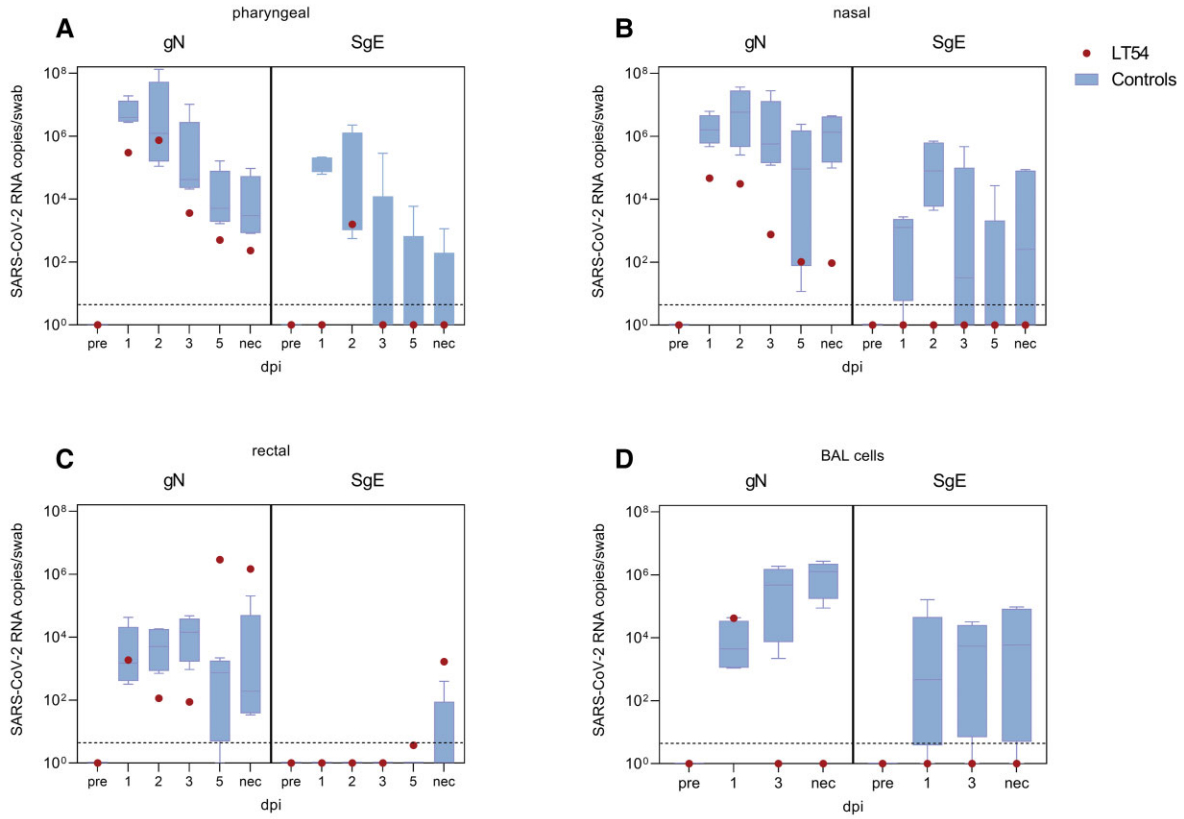

Figure 1. RT-qPCR assessed viral RNA loads post SARS-CoV-2 challenge. Viral RNA was quantified for SARS-CoV-2 genomic N and subgenomic E content in pharyngeal, nasal, and rectal swabs (*A*, *B*, and *C*, respectively) and BAL cells (*D*). Lines are median values, boxes are 25th to 75th percentiles, and whiskers are minimum and maximum values. Abbreviations: BAL, bronchoalveolar lavage; dpi, days postinfection; nec, necropsy; pre, preexposure; RT-qPCR, real-time quantitative polymerase chain reaction; SARS-CoV-2, severe acute respiratory syndrome coronavirus 2.

RNA in all sites except the duodenum. The highest levels were seen in the jejunum and descending colon (Supplementary Figure 1B), potentially indicating preferential replication in those sites, although this could be related to sampling error rather than biological preference. The ileum of LT54 showed minimal changes upon infection (Supplementary Figure 1C), despite positive viral staining via immunofluorescence (Supplementary Figure 1D).

Intrahost viral evolution is of interest due to the continued appearance of variants of concern throughout the pandemic. We sequenced virus at each site it was present to determine evolutionary patterns present in LT54 during this study. Present in our challenge inoculum at low levels were deletions in the furin cleavage site that disappeared during challenge, as has been seen before [13–15], presumably due to lack of replication favorability. The H655Y and N149K changes were seen in the jejunum and transverse colon (Figure 2). H655Y has been reported before in a primate model of SARS-CoV-2 infection, with the change being near the furin cleavage site likely favoring increased replication [15]. N149K is found in the N-terminal domain of spike protein, in an area less well characterized than RBD. This site is not targeted by the antibodies administered, so is unlikely to have arisen due to this prophylactic approach. Rather, this is more likely reflective of the low dose of antibody administered, as well as a more rapidly decreasing antibody level in LT54 than in others of the same low-dose cohort. Interestingly, the sequences seen in the descending colon and rectum were identical to the WA1/2020 isolate (Figure 2).

DISCUSSION

Here, we present data from 1 animal that was challenged with SARS-CoV-2 after prophylactic administration of combination anti-spike antibody therapy. Despite robust respiratory protection afforded using this antibody combination, high viral loads were observed in the intestinal mucosa. In addition, sequence changes were present indicating increased replication, as well as site-specific changes that may indicate increased replication at those sites, allowing for those evolutionary patterns to emerge. Finally, we consider the disappearance of the furin cleavage site deletion present in the challenge inoculum to be further evidence of the importance of an intact furin cleavage site in the in vivo infection and replication of SARS-CoV-2.

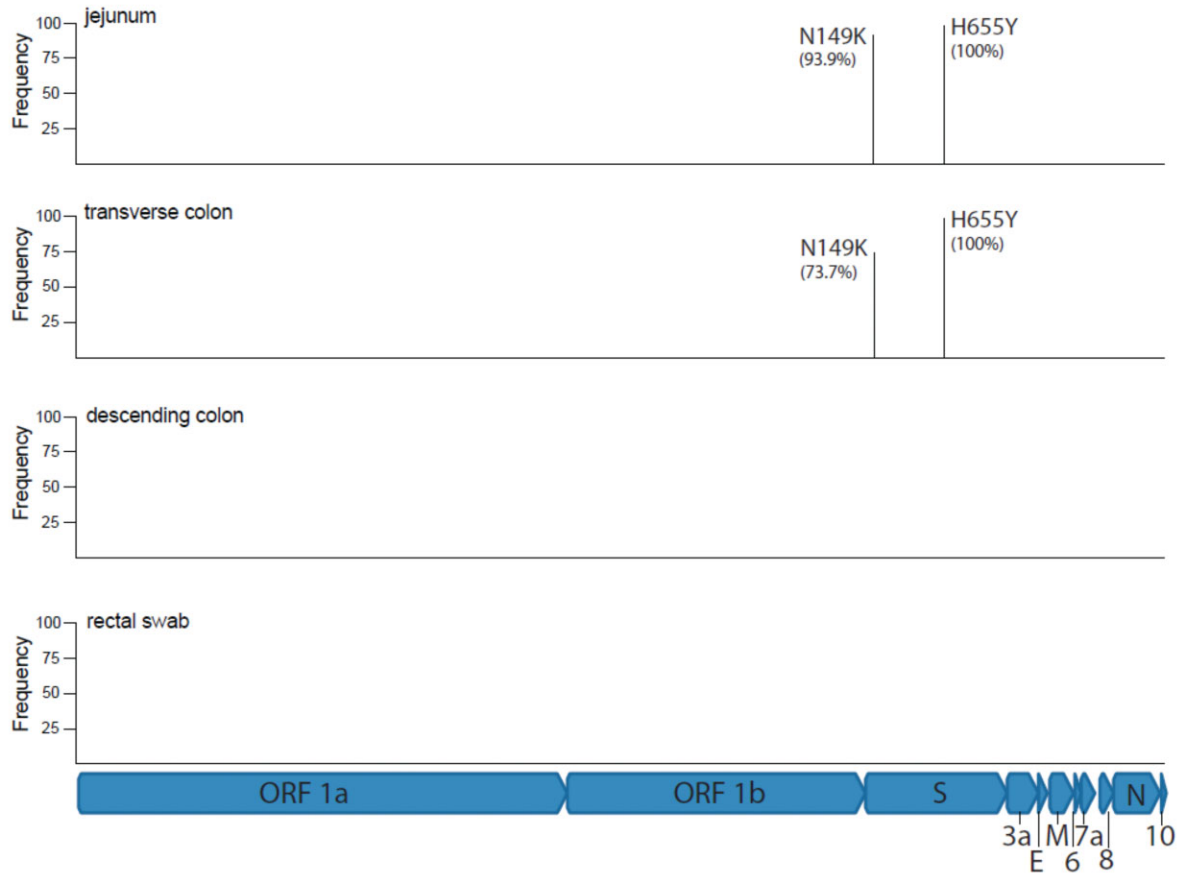

Figure 2. Sequence changes found in gastrointestinal sites of LT54 after SARS-CoV-2 challenge. Viral RNA was sequenced at anatomical sites indicated, with frequency and amino acid substitutions relative to the WA1/2020 patient isolate, with their relative frequency within the sample noted. Abbreviations: ORF, open reading frame; SARS-CoV-2, severe acute respiratory syndrome coronavirus 2.

Further work may include adapting these sequence changes into current circulating strains to determine the effect, if any, on replication and pathogenesis in vivo.

Supplementary Data

Supplementary materials are available at *The Journal of Infectious Diseases* online (http://jid.oxfordjournals.org/). Supplementary materials consist of data provided by the author that are published to benefit the reader. The posted materials are not copyedited. The contents of all supplementary data are the sole responsibility of the authors. Questions or messages regarding errors should be addressed to the author.

Notes

Acknowledgments. We thank Dr Michel Nussenzweig for provision of the critical reagent monoclonal antibodies for this evaluation. We also acknowledge and thank Drs Clint Florence, Jean Patterson, Que Dang, and Nancy Miller all at NIH/NIAID for invaluable scientific input on the study, and critical review of the manuscript. We thank Ms Nadia Golden, Breeana Picou, Skye Spencer, and Krystal Hensley all members of the TNPRC High Containment Performance Core for their work. We thank Angela Birnbaum for reviewing and optimizing all technical SOPs and overseeing the safety of this study.

Financial support. This work was supported, in part, by National Institute of Allergy and Infectious Disease (contract number HHSN272201700033I to C. J. R.); and National Institutes of Health Office of Research Infrastructure Programs, Office of the Director (grant number OD011104).

Potential conflicts of interest. All authors: No reported conflicts. All authors have submitted the ICMJE Form for Disclosure of Potential Conflicts of Interest. Conflicts that the editors consider relevant to the content of the manuscript have been disclosed.

References

1. Harvey WT, Carabelli AM, Jackson B, et al. SARS-CoV-2 variants, spike mutations and immune escape. Nat Rev Microbiol **2021**; 19:409–24.

2. Weinreich DM, Sivapalasingam S, Norton T, et al. REGN-COV2, a neutralizing antibody cocktail, in outpatients with Covid-19. N Engl J Med **2021**; 384:238–51.
3. Robbiani DF, Gaebler C, Muecksch F, et al. Convergent antibody responses to SARS-CoV-2 in convalescent individuals. Nature **2020**; 584:437–42.
4. Beddingfield BJ, Maness NJ, Fears AC, et al. Effective prophylaxis of COVID-19 in Rhesus macaques using a combination of two parenterally-administered SARS-CoV-2 neutralizing antibodies. Front Cell Infect Microbiol **2021**; 11:753444.
5. Van Rompay KKA, Olstad KJ, Sammak RL, et al. Early treatment with a combination of two potent neutralizing antibodies improves clinical outcomes and reduces virus replication and lung inflammation in SARS-CoV-2 infected macaques. PLoS Pathog **2021**; 17:e1009688.
6. Xiao F, Tang M, Zheng X, Liu Y, Li X, Shan H. Evidence for gastrointestinal infection of SARS-CoV-2. Gastroenterology **2020**; 158:1831–3.e3.
7. Ma C, Cong Y, Zhang H. COVID-19 and the digestive system. Am J Gastroenterol **2020**; 115:1003–6.
8. Yantiss RK, Qin L, He B, et al. Intestinal abnormalities in patients with SARS-CoV-2 infection: histopathologic changes reflect mechanisms of disease. Am J Surg Pathol **2022**; 46:89–96.
9. Pan L, Mu M, Yang P, et al. Clinical characteristics of COVID-19 patients with digestive symptoms in Hubei, China: a descriptive, cross-sectional, multicenter study. Am J Gastroenterol **2020**; 115:766–73.
10. Mlcochova P, Kemp SA, Dhar MS, et al. SARS-CoV-2 B.1.617.2 Delta variant replication and immune evasion. Nature **2021**; 599:114–9.
11. Lucas C, Vogels CBF, Yildirim I, et al. Impact of circulating SARS-CoV-2 variants on mRNA vaccine-induced immunity. Nature **2021**; 600:523–9.
12. Greaney AJ, Loes AN, Crawford KHD, et al. Comprehensive mapping of mutations in the SARS-CoV-2 receptor-binding domain that affect recognition by polyclonal human plasma antibodies. Cell Host Microbe **2021**; 29:463–76.e6.
13. Sasaki M, Toba S, Itakura Y, et al. SARS-CoV-2 bearing a mutation at the S1/S2 cleavage site exhibits attenuated virulence and confers protective immunity. mBio **2021**; 12: e0141521.
14. Lau SY, Wang P, Mok BW, et al. Attenuated SARS-CoV-2 variants with deletions at the S1/S2 junction. Emerg Microbes Infect **2020**; 9:837–42.
15. Rowe LA, Beddingfield BJ, Goff K, et al. Intra-host SARS-CoV-2 evolution in the gut of mucosally-infected *Chlorocebus aethiops* (African Green Monkeys). Viruses **2022**; 14:77.